

## Dipole–dipole interaction in square arrays of MnAs nanodisks on GaAs(001)

This article has been downloaded from IOPscience. Please scroll down to see the full text article.

2008 J. Phys.: Condens. Matter 20 225007

(<http://iopscience.iop.org/0953-8984/20/22/225007>)

View [the table of contents for this issue](#), or go to the [journal homepage](#) for more

Download details:

IP Address: 129.252.86.83

The article was downloaded on 29/05/2010 at 12:30

Please note that [terms and conditions apply](#).

# Dipole–dipole interaction in square arrays of MnAs nanodisks on GaAs(001)

Y Takagaki, C Herrmann and E Wiebicke

Paul-Drude-Institut für Festkörperelektronik, Hausvogteiplatz 5-7, 10117 Berlin, Germany

Received 3 October 2007, in final form 12 February 2008

Published 16 April 2008

Online at [stacks.iop.org/JPhysCM/20/225007](http://stacks.iop.org/JPhysCM/20/225007)

## Abstract

We demonstrate dipolar correlation in the orientation of magnetization in square arrays of MnAs nanodisks fabricated from epitaxial layers on GaAs(001). The MnAs(1 $\bar{1}$ 00) layers possess strong in-plane uniaxial magnetocrystalline anisotropy, which enables us to discard microvortex-type ordering from degeneracy while maintaining the disks as circularly shaped with a small diameter. The autocorrelation function reveals antiferromagnetic collinear arrangements of the magnetic moments in the arrays both in the single-domain and flux-closure-state regimes of the disks. The interaction range is deduced to be nearly identical to the period of the arrays.

## 1. Introduction

In an ensemble of noncontacting magnetic dots, the dipole–dipole interaction plays an important role in the magnetic properties. Prakash and Henley [1] theoretically examined the ground state of infinite square and hexagonal lattices by restricting the interaction to the nearest neighbors. The interaction was shown to produce the two types of configuration illustrated in figure 1(a). (We do not distinguish between a collinear configuration and its 90°-rotated one.) They form continuously degenerate ground states at temperature  $T = 0$  [2], while a particular state is favored by perturbations that occur in realistic situations. Due to the subtle nature of the ground state, the predictions, however, need to be regarded with caution as the dipole–dipole interaction is, in reality, long ranged [3].

In numerical calculations based on a finite system, the dipole–dipole interaction can be fully taken into account [4–8]. However, the lattice truncation at the boundaries influences the ordering significantly, as the outer magnetic moments tend to be aligned along the border to reduce stray magnetic fields. As an example, we show in figure 1(b) a numerical result of a nearly demagnetized state in a two-dimensional square lattice with the size  $N = 15$ . The magnetic moments, which were initially oriented randomly, were set to rotate under the dipolar interaction until a quasistable state had been realized [7]. The configuration thus corresponds approximately to the ordering in a thermally demagnetized state. The interaction is found to be as evident in the demagnetized state as in the remanence state examined in [7]. The arrangement of the magnetic moments can be understood as a mixture of the collinear

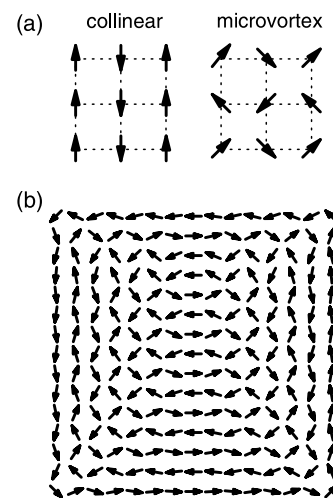


**Figure 1.** (a) Collinear and microvortex configurations of ordering resulting from dipole–dipole interaction. (b) Nearly demagnetized state when the size of the square array is  $N = 15$ . A quasistable state was realized through dipole–dipole interaction from an initial configuration where the magnetic moments were randomly oriented.

and microvortex configurations. The strong influences of the boundary are also apparent.

Testing the magnetic orderings in experimental systems [9–11] is of great interest not only from the viewpoint of fundamental physics but also for applications, including magneto-logic devices [12]. However, there exists an obstacle in realizing the ordering using microstructured dipolar magnets. That is, the magnetocrystalline and shape anisotropies

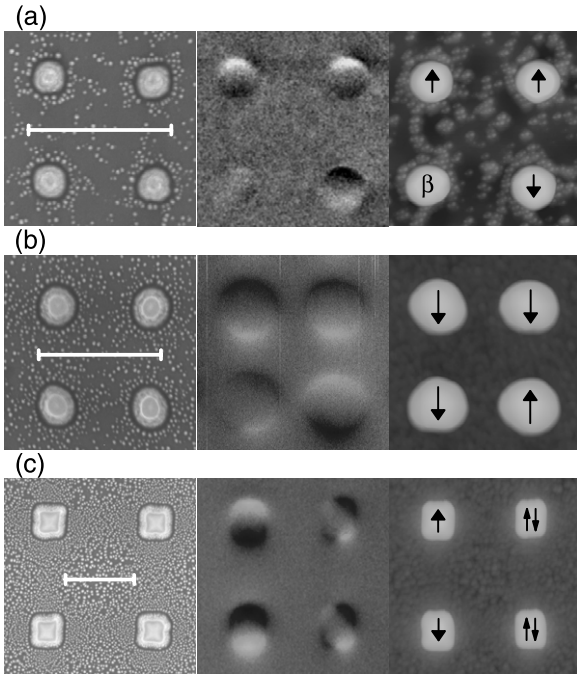


**Figure 2.** Images of arrays of MnAs disks (a) 1a, (b) 2a, and (c) 2b taken from left to right using, respectively, scanning-electron, magnetic-force, and atomic-force microscopies at a temperature of about 20 °C. The scale bars indicate a length of 500 nm. The arrows indicate the direction of magnetization. The disk marked ‘ $\beta$ ’ is composed mostly of the nonmagnetic  $\beta$ -MnAs. The [11 $\bar{2}$ 0] and [0001] directions of MnAs layers are oriented along the vertical and horizontal directions, respectively.

dominantly determine the orientation of the magnetic moments, and so the influences of the dipole–dipole interaction are hard to recognize [9, 10]. The degeneracy and/or mixture of the collinear and microvortex configurations are also troublesome as, for quantitative evaluation of long-range ordering, unambiguous discrimination between them is required. Hampered by these difficulties, the dipole–dipole interaction has been manifested so far, in principle, only between two closely neighboring disks [12–14]. The coupling between disks, which were elongated to fix the direction of the magnetization axis [12, 14], has been demonstrated as a way to construct magneto-logic devices. We also note that Novosad *et al* [11] revealed the role of the interaction in the reversal processes of the magnetization in an array of densely packed multi-domain disks.

In this paper, we investigate the ordering due to the dipole–dipole interaction in square arrays composed of small ferromagnetic disks fabricated from epitaxial MnAs layers on GaAs(001). We focus our attention on seeking the evidence for dipole–dipole interaction in the previously unsuccessful regime, where the diameter of the disks is negligibly small in comparison to the period of the arrays. We employ MnAs to take advantage of its strong uniaxial magnetocrystalline anisotropy [15], i.e., the shape anisotropy is overwhelmed by the magnetocrystalline anisotropy [16, 17]. In addition, the atomic magnetic moments within a MnAs disk are fairly rigidly aligned along the magnetic easy axis, thereby

**Table 1.** Parameters of three samples and results of magnetic-force-microscopy analysis of the magnetic state in the disks. The thickness  $t$  and diameter  $d$  of the MnAs disks and the period  $a$  of the square arrays are listed.  $n_{\uparrow}$ ,  $n_{\downarrow}$ , and  $n_{\uparrow\downarrow}$  are the numbers of the disks having upward-, downward-, and antiparallel-oriented magnetization, respectively. The polarization  $p$  was calculated using these numbers. The number of disks invisible in the magnetic imaging is  $n_{\beta}$ .

Sample	$t$ (nm)	$d$ (nm)	$a$ (nm)	$n_{\uparrow}$	$n_{\downarrow}$	$n_{\uparrow\downarrow}$	$n_{\beta}$	$p$
1a	37	60	350	44	34	0	11	0.13
2a	50	100	380	30	10	2	8	0.48
2b	50	170	750	13	10	20	1	0.07

maintaining the magnetization of an individual disk to be nearly as large as the bulk value. In a disk prepared from a nearly isotropic material, in contrast, the net magnetization is reduced significantly due to meandering of the atomic magnetic moments, which is similar to the tilting of the boundary magnetic moments in figure 1(b). The uniaxial anisotropy implies that the collinear configuration is favored over the microvortex configuration, allowing us to circumvent the coexistence of the two types of ordered configurations. We manifest the collinear ordering by evaluating autocorrelation of the orientations of the magnetization in the MnAs arrays. We observe a rapid decay of the correlation. The length of correlation is a crucial parameter for magneto-logic devices as it determines the degree of ‘cross-talk’ between logic elements.

## 2. Experimental details

MnAs is a room-temperature ferromagnetic material that can be grown epitaxially on substrates like GaAs and Si. These properties make it attractive for spintronic applications. In bulk MnAs, the magnetic hard axis is oriented along the  $c$ -axis of the hexagonal crystal and the  $C$ -plane is the magnetic easy plane. Epitaxial MnAs layers grow on GaAs(001) substrates with the  $c$ -axis being laid in the surface plane. The magnetocrystalline anisotropy is, as a consequence, uniaxial and markedly strong. For the present study, we grew two MnAs layers using molecular-beam epitaxy at a growth temperature of 230 °C [18]. The growth rate was 15 and 10 nm h<sup>-1</sup> for layers 1 and 2, respectively. The magnetization in the films flipped at about 0.6 kOe when external magnetic field was applied along the magnetic easy axis, whereas the magnetic field required to align the magnetization along the magnetic hard axis, i.e. to tilt the magnetization in-plane by 90°, was as large as 19 kOe. The uniaxial anisotropy constant deduced for similar layers was  $K \sim 1 \times 10^6$  J m<sup>-3</sup> [19], which is one order of magnitude larger than that in Fe. Microstructuring was carried out by means of electron-beam lithography and Ar ion milling [20]. Nanometer-scale disks were assembled in the form of a square array. In the left-hand column in figure 2 we show scanning-electron micrographs of devices. In table 1 we list the thickness  $t$  of the epitaxial layers, the diameter  $d$  of the disks, and the period  $a$  of the arrays for the three samples we investigate below. The structural parameters were chosen to fulfill the condition  $d \ll a$ .

### 3. Magnetic and structural states in MnAs disks

The magnetic state in the disks was examined using magnetic-force microscopy (MFM) at room temperature (about 20 °C). The MFM images taken from the three devices are shown in the middle column in figure 2. Here, the magnetic easy axis is oriented in the vertical direction. The MFM tip was positioned in such a way as to detect a magnetic field normal to the surface. An in-plane magnetic moment in the disks, therefore, yields a combination of bright and dark contrasts in the sections where the magnetic field associated with the moment is directed away from and toward the surface, respectively. We indicate the direction of the magnetic moments by the arrows in the corresponding atomic-force micrographs shown in the right-hand column in figure 2. Owing to the large value of  $KV/k_B T$  ( $= 10^4$ – $10^5$ ) in the MnAs disks, the thermal agitation was negligible. Here,  $V$  is the volume of the disk and  $k_B T$  is the thermal energy [15]. The interaction between the MFM tip and the disks was also negligibly small to flip the magnetization orientation during the scanning of the tip. The MFM images were taken twice from about half of the disks. The images were completely reproducible as far as the magnetization orientation was concerned. The stability is expected as the coercive field of the MnAs disks (about 0.7 kOe) is large [15].

In identifying the magnetic states, one needs to be aware of two phenomena that occur in MnAs disks on GaAs(001). First, the disks undergo a transition from the single-magnetic-domain state to the flux-closure state when  $d$  exceeds a critical value [21]. The transition to the flux-closure state is driven by a gain in the magnetostatic energy due to the suppressed stray magnetic fields. The flux-closure state is, however, unfavorable in small disks due to the cost of the domain-wall energy. The critical diameter for the present layer thicknesses is between 100 and 170 nm. We, consequently, find that most of the disks in samples 1a ( $d = 60$  nm) and 2a ( $d = 100$  nm) contain no more than one magnetic domain even in a demagnetized state. The disks in sample 2b are, in contrast, composed of two magnetic moments, which are oriented practically randomly to each other. Note that all the magnetic moments in figure 2 are oriented in the vertical direction due to the strong uniaxial magnetocrystalline anisotropy. The vortex state does not occur in MnAs disks on GaAs(001). This leads to an advantageous feature of MnAs disks in exploring the ordering due to the dipole–dipole interaction; i.e., the magnetization in an individual disk is maintained to be as large as in bulk MnAs.

Second, a simultaneous magnetic and structural phase transition takes place in MnAs at a Curie temperature of  $T_C \approx 40$  °C. The transition between the ferromagnetic  $\alpha$  phase and the nonmagnetic  $\beta$  phase<sup>1</sup> is first order, i.e., it takes place when the potential barrier separating the two phases is surmounted. As a consequence of the nucleation initiation of the first-order phase transition, two kinds of disks consisting of either  $\alpha$ - or  $\beta$ -MnAs coexist in a wide temperature range around  $T_C$  [17]. An

example is found in figure 2(a), in which the lower left disk is invisible in the MFM image. The disappearance indicates that the disk is entirely composed of  $\beta$ -MnAs, although the MFM image was obtained at a temperature considerably lower than  $T_C$ .

We have mapped out the magnetic states in a large number of disks following demagnetization of the devices by a heating to about 60 °C. The MFM observations were carried out in the central portion of arrays with  $N$  being a few hundred. The boundary effects for the finite arrays are thus negligibly small. The results are summarized in table 1, where  $n_\uparrow$  and  $n_\downarrow$  are the number of disks having a single magnetic domain with the orientation of the magnetization being upward and downward, respectively. That  $n_\uparrow \approx n_\downarrow$  in 1a and 2b confirms that these devices were indeed demagnetized. The number of disks exhibiting two antiparallel magnetic moments is  $n_{\uparrow\downarrow}$ ,<sup>2</sup> and  $n_\beta$  is the number of disks composed solely of  $\beta$ -MnAs. One finds in table 1 that  $n_{\uparrow\downarrow}$  decreases and  $n_\beta$  increases with reducing  $d$ . The latter originates from the fact that core–shell-type phase coexistence is permitted within an individual disk when the disks are relatively large [17]. The phase transition between the  $\alpha$  and  $\beta$  phases involves an abrupt expansion of the lattice constant along the  $a$  axis. The strain imposed by the substrates makes the phase coexistence favorable. The coexistence is known in epitaxial layers on GaAs(001) to occur by repeating submicrometer-wide strips of  $\alpha$ - and  $\beta$ -MnAs in the MnAs[11 $\bar{2}$ 0] direction [18].

### 4. Ordering due to dipole–dipole interaction

In order to verify the presence of ordering in the distribution of the magnetization orientation, we have evaluated the autocorrelation function

$$C(m, n) = \langle \sigma(i, j) \sigma(i + m, j + n) \rangle_{i, j}, \quad (1)$$

where  $\sigma(i, j) = 1$  and  $-1$  when the magnetization in the disk located at  $(i, j)$  is top and bottom oriented, respectively. The averages regarding  $i$  and  $j$  are taken in the directions of magnetic hard and easy axes, respectively. The disks containing the antiparallel magnetic moments ( $n_{\uparrow\downarrow}$ ) and  $\beta$ -MnAs ( $n_\beta$ ) were treated as vacancies [23] and excluded from the correlation analysis. We again emphasize that the microvortex configuration is disfavored by the uniaxial magnetocrystalline anisotropy, and so we have focused our attention on detecting the collinear ordering. For perfect collinear arrangements, one obtains  $C(m, n) = (-1)^m$ . In a real system,  $C(m, n)$  is anticipated to approach zero when  $m$  or  $n$  increases due to disorder.

We plot  $C(m, n)$  in figure 3 for  $n = 0$  (filled circles) and 1 (open circles). As the devices were not in the ideal demagnetized state in reality, the autocorrelation should remain finite ( $=p$ ) even in the absence of correlation. Here, the polarization

$$p = \frac{n_\uparrow - n_\downarrow}{n_\uparrow + n_\downarrow + n_{\uparrow\downarrow}} \quad (2)$$

<sup>1</sup> Although  $\beta$ -MnAs is generally considered to be paramagnetic, there has been a debate that  $\beta$ -MnAs may be antiferromagnetic. See [22] and the references therein. In either case, the disks consisting solely of  $\beta$ -MnAs can be ignored for the ordering induced by the dipole–dipole interaction.

<sup>2</sup> When the antiparallel double magnetic domains were considerably different in their volumes, the magnetic fields arising from the smaller domain were insignificant. These disks were hence counted as single-domain disks with the orientation of magnetization being in the dominant direction.

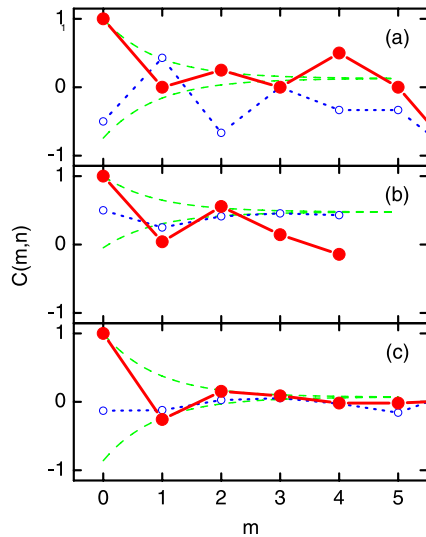


**Figure 3.** Autocorrelation function  $C(m, n)$  for the square arrays of MnAs disks (a) 1a, (b) 2a, and (c) 2b. The displacements  $m$  and  $n$  are along the directions of the magnetic hard and easy axes, respectively. The filled and open circles correspond to  $n = 0$  and  $1$ , respectively. The dashed curves show a decay when the correlation length is  $\xi = 0.9a$ .

(This figure is in colour only in the electronic version)

represents the degree of magnetization of the arrays. The value of  $p$  is indicated in figure 3 by the dashed curves in the limit of  $m \rightarrow \infty$ . In all three plots,  $C(1, 0)$  and  $C(2, 0)$  are smaller and larger than  $p$ , respectively. (Note that  $C(0, 0) = 1$  by definition.) The presence of a collinear ordering in the easy axis direction is, therefore, evidenced. No appreciable difference was found between the disks in the single-domain regime (1a and 2a) and flux-closure regime (2b), as the analysis relies on the disks exhibiting a single magnetic moment. We note that the statistical errors increase significantly for large  $m$ . The behavior for  $m \geq 3$  is likely to be affected by the statistical uncertainties. We emphasize that the presence of the antiferromagnetic collinear ordering can be, nevertheless, safely deduced from the behavior for  $m = 1$  and  $2$ .

Such a systematic variation of  $C$  for  $m = 0, 1$ , and  $2$  is not found when  $n = 1$ . We may estimate the correlation length  $\xi$  assuming a decay  $\pm(1 - p) \exp(-ma/\xi) + p$  for  $C(m, 0)$ . The dashed curves in figure 3 show fits assuming  $\xi = 0.9a$ . The small value of  $\xi$  is consistent with the fact that the collinear ordering was below the experimental detection limit for  $n = 1$ . The common features of the autocorrelation function between the three devices indicating the presence and absence of ordering, respectively, for  $n = 0$  and  $1$  attest the statistical certainty. It is noteworthy that approximating the dipole–dipole interaction to the nearest neighbors can thus be justified in our samples. The boundary effects can also be disregarded in the experimental systems, unless the correlation length is drastically improved. As the correlation length is fairly similar in the three devices despite the considerable difference in  $d$  and  $a$ , structural imperfections associated with the microstructuring may be suggested to be the main source of the disorder. As indicated by the clear experimental demonstrations in [12–14], the ordering of magnetic moments

due to one-dimensional dipole–dipole interaction is robust in comparison to that due to two-dimensional interaction. The fluctuations in the inter-disk spacing will thus result in a local ordering between closely neighboring disks. The correlation length being close to the lattice constant might imply that the ordering in our square arrays is, in principle, dominated by the two-object interaction.

The magnetic field  $\mathbf{H}$  at the position  $\mathbf{r}$  induced by a dipole moment  $\mathbf{m}$  is given by

$$\mathbf{H}(\mathbf{r}) = \frac{1}{4\pi} \frac{3(\mathbf{m} \cdot \mathbf{r})\mathbf{r} - \mathbf{m}r^2}{r^5}. \quad (3)$$

For the collinear ordering, the magnetic field acting on a disk arising from the rest of the disks is along the magnetic easy axis and amounts to  $0.41MV/a^3$ . For our devices, we find values that are on the order of 10 Oe. The field when the magnetization is ferromagnetically aligned is  $0.36MV/a^3$ , which is smaller than that for the antiferromagnetic collinear ordering. While the difference in the field strength is appreciable, the rather small difference suggests that the energies of various order states may lie within the thermal energy at room temperature with respect to the ground-state energy. Therefore, the thermal demagnetization may not be able to produce the antiferromagnetic collinear ordering without intrusion of the ferromagnetic collinear and other orderings. This may provide an alternative explanation for the short correlation.

The ordering due to dipole–dipole interaction was suggested in the relaxation of the magnetization of magnetized arrays [24]. In the nearly magnetized state, the magnetic moments in the four nearest neighbors of a disk are ferromagnetically aligned, in contrast to the antiferromagnetic ordering in the demagnetized state. The dipole–dipole interaction is hence expected to entice a ferromagnetic alignment in the center disk. From the amount of anomalous increase of the magnetization observed in the magnetization relaxation measurements in [24], the magnitude of the influence of the dipole–dipole interaction is roughly estimated to be about 1%. The small variation is reasonable considering the rather strong decay of the dipolar correlation revealed in figure 3.

## 5. Conclusion

In conclusion, we have investigated the ordering due to dipole–dipole interaction in square arrays composed of nanometer-scale ferromagnetic disks in the regime where the diameter of the disks is considerably smaller than the period of the array, i.e., the disks can be regarded as point-like magnetic moments. We have employed epitaxial MnAs layers on GaAs(001) in preparing the devices in order to overcome the shape anisotropy by exploiting the strong uniaxial magnetocrystalline anisotropy. We have revealed collinear arrangements of the magnetic moments among the disks by evaluating the autocorrelation function. The decay of the correlation indicates that the interaction is restricted almost to the nearest neighbors in our devices. The short correlation may originate from the positioning imperfection in the array assembly and/or the

rather small energy difference between the antiferromagnetic and ferromagnetic collinear orderings.

## References

- [1] Prakash S and Henley C L 1990 *Phys. Rev. B* **42** 6574
- [2] Zimmerman G O, Ibrahim A K and Wu F Y 1988 *Phys. Rev. B* **37** 2059
- [3] Guslienko K Y 1999 *Appl. Phys. Lett.* **75** 394
- [4] Chang C and Fredkin D R 1986 *IEEE Trans. Magn.* **22** 391
- [5] Stamps R L and Camley R E 1999 *Phys. Rev. B* **60** 11694
- [6] Kayali M A and Saslow W M 2004 *Phys. Rev. B* **70** 174404
- [7] Takagaki Y and Ploog K H 2005 *Phys. Rev. B* **71** 184439
- [8] Ortigoza M A, Klemm R A and Rahman T S 2006 *Phys. Rev. B* **74** 226401
- [9] Grimsditch M, Jaccard Y and Schuller I K 1998 *Phys. Rev. B* **58** 11539
- [10] Abraham M C, Schmidt H, Savas T A, Smith H I, Ross C A and Ram R J 2001 *J. Appl. Phys.* **89** 5667
- [11] Novosad V, Guslienko K Y, Shima H, Otani Y, Kim S G, Fukamichi K, Kikuchi N, Kitakami O and Shimada Y 2002 *Phys. Rev. B* **65** 060402
- [12] Imre A, Csaba G, Ji L, Orlov A, Bernstein G H and Porod W 2006 *Science* **311** 205
- [13] Cowburn R P and Welland M E 2000 *Science* **287** 1466
- [14] Wang R F, Nisoli C, Freitas R S, Li J, McConville W, Cooley B J, Lund M S, Samarth N, Leighton C, Crespi V H and Schiffer P 2006 *Nature* **439** 303
- [15] Takagaki Y, Herrmann C, Wiebicke E, Herfort J, Däweritz L and Ploog K H 2006 *Appl. Phys. Lett.* **88** 032504
- [16] Takagaki Y, Wiebicke E, Hesjedal T, Kostial H, Herrmann C, Däweritz L and Ploog K H 2003 *Appl. Phys. Lett.* **83** 2895
- [17] Takagaki Y, Jenichen B, Herrmann C, Wiebicke E, Däweritz L and Ploog K H 2006 *Phys. Rev. B* **73** 125324
- [18] Däweritz L 2006 *Rep. Prog. Phys.* **69** 2581
- [19] Schippan F, Behme G, Däweritz L, Ploog K H, Dennis B, Neumann K-U and Ziebeck K R A 2000 *J. Appl. Phys.* **88** 2766
- [20] Takagaki Y, Wiebicke E, Däweritz L and Ploog K H 2006 *J. Solid State Chem.* **179** 2271
- [21] Jubert P-O and Allenspach R 2004 *Phys. Rev. B* **70** 144402
- [22] See Takagaki Y, Däweritz L and Ploog K H 2007 *Phys. Rev. B* **75** 035213 and the references therein
- [23] De'Bell K, MacIsaac A B, Booth I N and Whitehead J P 1997 *Phys. Rev. B* **55** 15108
- [24] Takagaki Y, Herfort J, Däweritz L and Ploog K H 2006 *Phys. Rev. B* **74** 224417